David A. Feinberg, Ph.D.
Catherine M. Mills, M.D.[2]
Jonathan P. Posin, M.D.
Douglas A. Ortendahl, Ph.D.
Nola M. Hylton, M.S.
Lawrence E. Crooks, Ph.D.
Jeffrey C. Watts, M.S.
Leon Kaufman, Ph.D.
Mitsuaki Arakawa, B.S.
John C. Hoenninger, M.S.E.E.
Michael Brant-Zawadzki, M.D.

Multiple Spin-Echo Magnetic Resonance Imaging[1]

Spin-echo magnetic resonance (MR) imaging detects a variety of pathologic states with great sensitivity. A technique for producing multiple spin-echo images in multisection operation is presented. This method of intensity-image acquisition is compared with retrospective intensity-image synthesis from routine data sets. Both yield long echo time (TE) images with similar image contrast and comparable and often increased diagnostic utility. Technical and clinical considerations are addressed, including signal-to-noise levels, flow effects, and patient throughput.

Index terms: Magnetic resonance, technology

Radiology 1985; 155: 437–442

IMAGES produced by magnetic resonance (MR) spin-echo techniques (1, 2) are useful in characterizing normal and diseased tissues. Previous investigators (3, 4) have explored the utility of multiple spin-echo imaging. Reported here is a versatile technique for producing multiple spin-echo images with repeated 180° radiofrequency (RF) refocusing pulses in multisection operation for clinical examinations.

Multisection spin-echo imaging by two-dimensional (2D) Fourier transform techniques (4) takes advantage of the fact that the time for magnetization recovery (T1 relaxation), typically 0.2–3.0 seconds (s) for protons, is greater than the time of a multiple spin-echo pulse sequence, which can range from 50 to 250 milliseconds (ms). During the recovery period of one section, which is the repetition time (TR) of the sequence, measurements from separate planar volumes in the subject are made without affecting the magnetization of the adjacent sections. This permits imaging of multiple sections without increasing imaging time above that needed for imaging one section (5).

Given the large number of possible echo times (TE) and echoes produced, there are a nearly infinite number of multiple-echo imaging techniques. However, trade-offs between the number of sections, number of echoes, and imaging time directly affect the clinical utility of any chosen technique. For example, 20 contiguous sections with two echoes at TE = 28 and 56 ms can be acquired in our imager in 17.1 minutes, while a maximum of 10 sections of multiple echoes up to 200 ms can be acquired in the same time with all other factors being equal (i.e., resolution, number of projections, and number of signal averages).

An alternative method for obtaining intensity images at late echo times is retrospective computer image processing of two spin-echo images with identical repetition times (TR) (6). Assuming that in the range where measured T2 decay is characterized by a single compartment model (monoexponential decay) in each image voxel, the two images are points on a T2 decay curve and can be used to extrapolate image intensity to earlier or later times. We compared the acquired spin-echo images with extrapolated spin-echo images, each at the same TR-TE combination, to study the additional T2 information produced by long TE imaging. The data base for this comparison was derived from clinical/pathologic conditions of the human brain, including infarction, primary and metastatic tumor, multiple sclerosis, and infection.

MATERIALS AND METHODS

The multiple spin-echo pulse sequence was developed and employed on a Diasonics MT/S imager operating at 0.35 T. In these experiments a series of five consecutive 180° RF pulses produced five spin-echo images at echo times of either 28, 56, 100, 150, and 200 ms, or 40, 80, 120, 160, and 200 ms. These five echo images were acquired on six contiguous sections (7.5 mm thick) using a selective volume RF irradiation technique. The RF pulses are applied with a frequency offset in the presence of a magnetic field gradient, resulting in spatially selective irradiations along the axis of the section selection gradient. This allows sections to undergo magnetization relaxation while other sections are being excited (4). A modified Carr-Purcell-Mei-

[1] From the Department of Radiology, Radiologic Imaging Laboratory, University of California, San Francisco, California. Received October 15, 1984; accepted and revision requested November 5; revision received November 15.

This study supported in part by Diasonics (MRI) Inc. and by USPHS grant CA32850 from the National Cancer Institute (DHHS).

[2] Current address: Diagnostic Networks Inc., San Francisco, California.

 db

boom-Gill (7) pulse sequence was used to alternate the phase of the RF pulse and to correct for possible accumulated errors in the 180° nutation. Intensity images were made by 2D Fourier transform (8) of the acquired data, with in-plane resolution of 1.7 × 1.7 mm.

In general, the total data acquisition time (t) of one multisection imaging sequence is the product of the TR time, the number of averages or repeated acquisitions of the data (n), and the number of lines in the image (N): $t = (TR)\ (n)\ (N)$. The number of sections (S) obtained in any one sequence is given by $S = TR/(TE_e + T_d)$, where TE_e is the echo time of the longest echo acquired and T_d is a delay time necessitated by certain instrument parameters. T_d incorporates delays to allow gradients to return to zero as well as to permit further magnetization decay from the sample volume selected. Certain imaging sequences may be more taxing on gradient power supply capabilities, and delays may need to be added to keep their duty cycle within reasonable limits. With increasing TR, more sections and/or more echoes can be acquired, possibly exceeding the ability of computer hardware or software to manage the data.

In this experiment, six adjacent sections were acquired, each with five spin echoes, TR = 1.5–2.5 s, TE_e = 200 ms, n = 4, and N = 128. With these values of TR and TE_e, the maximum possible number of sections that could be imaged (assuming negligible T_d) ranged from seven to 12. Because of software constraints, only six sections and a total of 30 images were obtained. Twenty patients with suspected intracranial pathology were imaged using the procedure described above, and 14 of the 20 were also imaged with our routine two-spin-echo sequence, TR = 0.5 and 2.0 s and TE = 28 and 56 ms. Diagnoses were confirmed with other imaging modalities as well as with histopathologic and clinical methods. By means of four different pairs of earlier echoes from the acquired five-echo intensity image data (echoes 1 and 2, 1 and 3, 1 and 4, and 2 and 3) and existing computational techniques (6), new intensity images were synthesized at anatomic planes of interest at TE times later than those actually used. Two of the researchers (C.M.M., J.P.P.) evaluated all images for quality, diagnostic utility, and increased specificity. To analyze changes in contrast between acquired and synthesized multiecho images, we sampled mean and standard deviation of the absolute intensity in areas of edema, normal surrounding tissue, and, where applicable, central areas of lesions. Contrast (C) was determined from $C = (L - B)/B$, where L and B are the mean intensity values of the lesion and its background, respectively. The standard error ΔC was determined from $\sqrt{[(\Delta L/B)^2 + (L \times \Delta B/B^2)^2]}$, where ΔL and ΔB represent the standard deviations of the measured values L and B.

ANALYSIS

The noise in the calculated image is directly proportional to the noise level in the acquired image data.[3] Noise in MR images is largely due to random currents in conductive tissue and electronic noise in the RF receiver components of the imaging system. The noise level in computer-generated images is proportional to the noise in the acquired images determined by the propagation of errors (9). In Figure 1 we compare the effects on signal-to-noise (S/N) ratios of calculations of new echoes from an acquired pair, TE = 28 and 56 ms. The results are shown as the ratio of S/N in the calculated image to S/N in the acquired image. At points between the two values, the S/N ratio improves because of data averaging in the two acquired echoes. Earlier calculated echoes have lower S/N ratios. An interesting effect is noted for late calculated echoes: the S/N ratio first decreases and then increases compared with the S/N ratio of the acquired images, the increase occurring sooner for tissues with

Figure 1

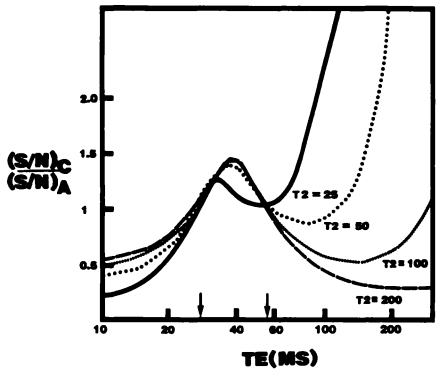

Ratio of S/N for calculated to S/N for acquired images for echoes calculated at different TE values (horizontal axis), starting with an echo pair at 28 and 56 ms (vertical arrows along TE axis). Results are shown for four T2 values that encompass the range of interest.

TABLE I: Contrast Evaluation

TE	Center vs. Edema			Edema vs. Normal		
	C	ΔC	C/ΔC	C	ΔC	C/ΔC
Acquired (TR = 2.5 s)						
28	0.213	0.093	2.29	0.569	0.102	5.57
56	0.387	0.156	2.48	0.992	0.188	5.27
100	0.812	0.251	3.23	1.56	0.266	5.86
150	1.39	0.500	2.78	3.78	1.26	3.00
200	1.64	0.604	2.71	4.68	1.58	2.96
Calculated (TR = 2.5 s)						
From 28/56						
100	0.705	0.324	2.17	1.89	0.459	4.11
150	1.14	0.616	1.85	3.43	1.05	3.26
200	1.68	1.05	1.60	5.71	2.11	2.70
From 28/100						
150	1.38	0.489	2.82	2.59	0.567	4.56
200	2.12	0.863	2.45	4.02	1.09	3.68
From 28/150						
200	2.15	0.846	2.54	6.47	2.64	2.45
From 56/100						
150	1.43	0.590	2.42	2.39	0.659	3.62
200	2.23	1.17	1.90	3.45	1.35	2.55

Note.—Contrast (C), standard error (ΔC), and detection confidence (C/ΔC) are compared for a patient with metastatic tumor (images seen in Fig. 2). Acquired images and images calculated from pairs of acquired images are evaluated for three regions. Contrast between the central tumor nidus and the edema, as well as between the edema and normal surrounding tissue, remains comparable when calculated images are compared with acquired images. While absolute contrast increases for longer TE times, detection confidence actually peaks at TE = 100 ms and falls thereafter.

TABLE II: Contrast Evaluation

TE	Center vs. Edema			Edema vs. Normal		
	C	ΔC	C/ΔC	C	ΔC	C/ΔC
Acquired (TR = 2 s)						
40	0.192	0.073	2.63	0.514	0.139	3.69
80	0.378	0.102	3.70	0.884	0.192	4.60
120	0.636	0.188	3.38	1.61	0.361	4.46
160	0.706	0.202	3.49	2.24	0.488	4.59
200	1.24	0.450	2.75	3.44	1.16	2.96
Calculated (TR = 2 s)						
From 40/80						
120	0.594	0.189	3.14	1.34	0.345	3.88
160	0.843	0.320	2.63	1.91	0.603	3.16
200	1.13	0.494	2.28	2.61	0.980	2.66
From 40/120						
160	0.915	0.301	3.04	2.42	0.657	3.68
200	1.24	0.451	2.74	3.47	1.12	3.09
From 40/160						
200	0.923	0.282	3.27	3.17	0.807	3.92
From 80/120						
160	0.937	0.345	2.71	2.59	0.829	3.12
200	1.29	0.565	2.29	3.89	1.69	2.30

Note.—Contrast (C), standard error (ΔC), and detection confidence (C/ΔC) are compared for a patient with infarction (images seen in Fig. 4). As before, contrast improves comparably for both acquired and calculated images as TE increases. Because of the increasing noise in both types of longer TE images, however, detection confidence actually peaks at TE = 100 ms and falls thereafter.

[3] Recent software and hardware changes have increased our image S/N ratios by 140%.

Figure 2

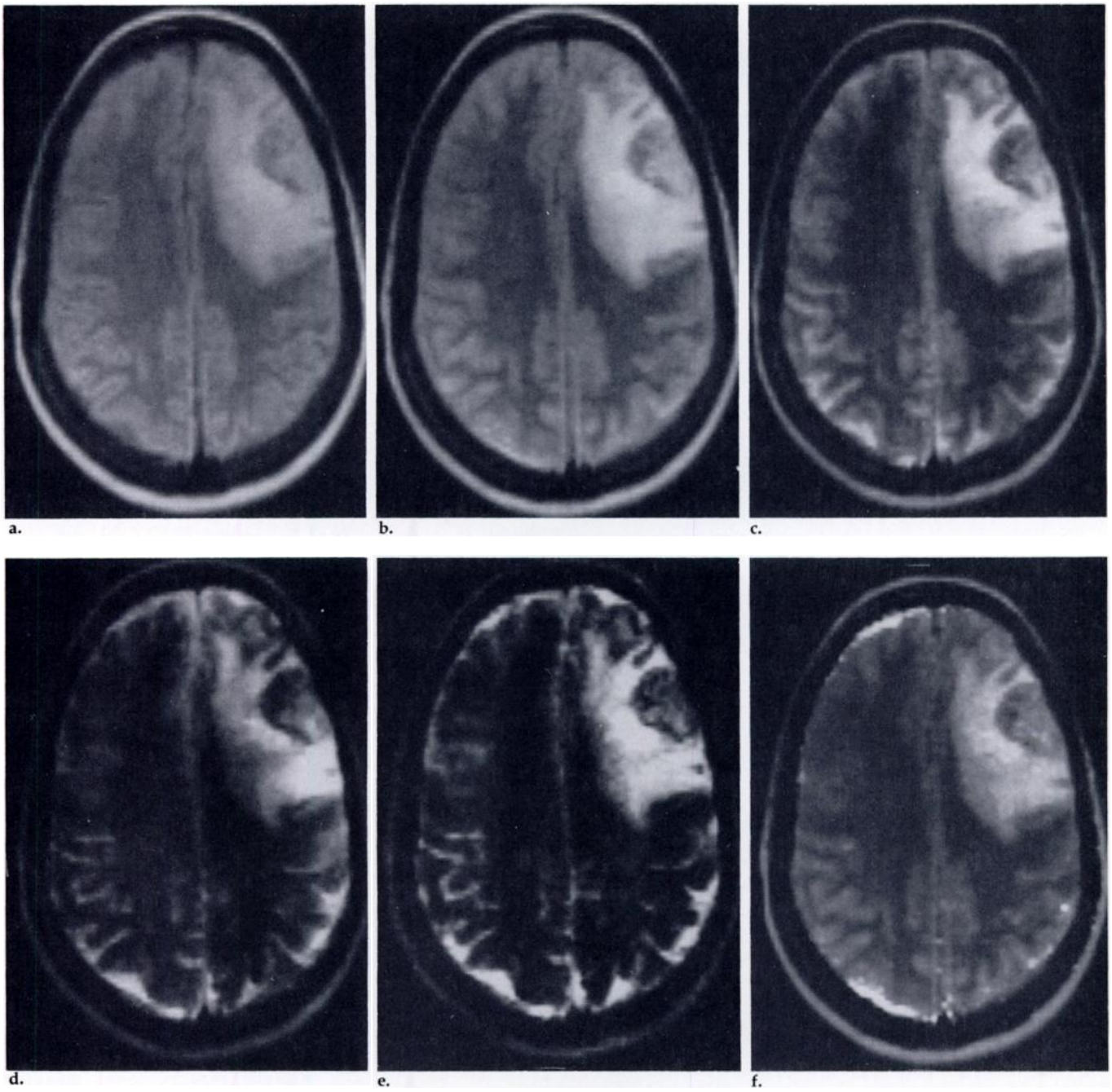

Metastatic melanoma. (**a**) TR = 2.5 s, TE = 28 ms; (**b**) TR = 2.5 s, TE = 56 ms; (**c**) TR = 2.5 s, TE = 100 ms; (**d**) TR = 2.5 s, TE = 150 ms: (**e**) TR = 2.5 s, TE = 200 ms; (**f**) integral; (**g**) average. Longer echo times accentuate contrast between the left frontal lobe metastasis and the adjacent edema. Integral and average images improve S/N ratio and overall contrast compared with any one echo.

smaller T2 values. This is because a late echo has little signal and a constant noise level for short T2. The TE = 28 and 56 ms images have stronger signals and the same level of noise, resulting in much higher S/N ratios. During calculation, there is a point along the TE axis where the decrease in the S/N ratio introduced by the calculation is less than the decrease in the S/N ratio introduced by T2 decay. Consequently, for T2 = 25 ms (near muscle), calculated late echoes are always better than acquired ones. For T2 = 50 ms (near brain), this crossover occurs at 120 ms. For pathologic tissues or cerebrospinal fluid (CSF), the crossover is much later. The effect, therefore, of calculations of late echoes on confidence (the ratio of contrast to its standard error) should be minimal, since normal tissues will have better S/N ratios in the calculated images than in the acquired images, and the pathologic tissues will have lower S/N ratios. When the two are summed to obtain ΔC, one term should partially compensate for the other, leading to comparable $C/\Delta C$ values in acquired and calculated late echoes.

RESULTS

Representative images are shown in Figures 2–6, and data on contrast calculations are in TABLES I and II. Intra-

cranial lesions were always detected using our standard TR = 2 s sequence, with two echoes at relatively short TE times of 28 and 56 ms. With the five-echo multisection sequence, lesions were equally well detected using earlier echoes of TE = 40 and 80 ms. In brain pathology where T2 is typically prolonged because of edema, echoes at longer TE times of up to 200 ms yielded increased contrast between lesions and their background, but poorer quality images resulted because of the decreased S/N ratio and the unclear distinction between gray and white matter. In patients with multicompartmental lesions, such as tumors, later echoes aided in the differentiation between tumor tissue and areas of edema (Fig. 2). Periventricular lesions, such as those in several of the patients with multiple sclerosis (Fig. 5), were often better imaged at intermediate or short TE times, because the relative intensity in CSF increases with TE and can efface the boundary between periventricular plaques and the ventricular system.

To retain the good anatomic resolution and S/N ratio of a short TE image while incorporating the excellent contrast between a lesion and its background seen in a long TE image, two approaches are possible (10). Utilizing a T2 map and a free induction decay (FID) image, both of which can be generated from early echoes taken from the multiecho image data, an integral image may be created (Fig. 2f). This image, a numerical product of the TE = 0 FID image and the T2 map, provides improved S/N ratio and overall contrast compared with any one late echo. Derived from the equation $S(\text{integral}) = S(0) \int_0^\infty \exp - (TE/T2)d(TE) = S(0) \times T2$ (where $S[0]$ is the signal at $TE = 0$), this integral image can be considered mathematically as an average of all possible TE times from zero to infinity. An even simpler method of postprocessing the multiple echoes involves simple numerical averaging of acquired echoes (Fig. 2g), which also provides improved S/N ratios. Both methods suffer from a slight loss of T2 information but may offer more optimal information while reducing the number of echoes to be evaluated.

Since the acquisition of later echoes reduces the number of section images that may be obtained during any one multiecho multisection sequence, the possibility of calculating new intensity images from pairs of earlier echoes was explored. The resulting synthesized images are seen in Figures 3, 4, and 6. Note that the overall image quality is good, with only a slight apparent increase in noise. The contrast between

Figure 3

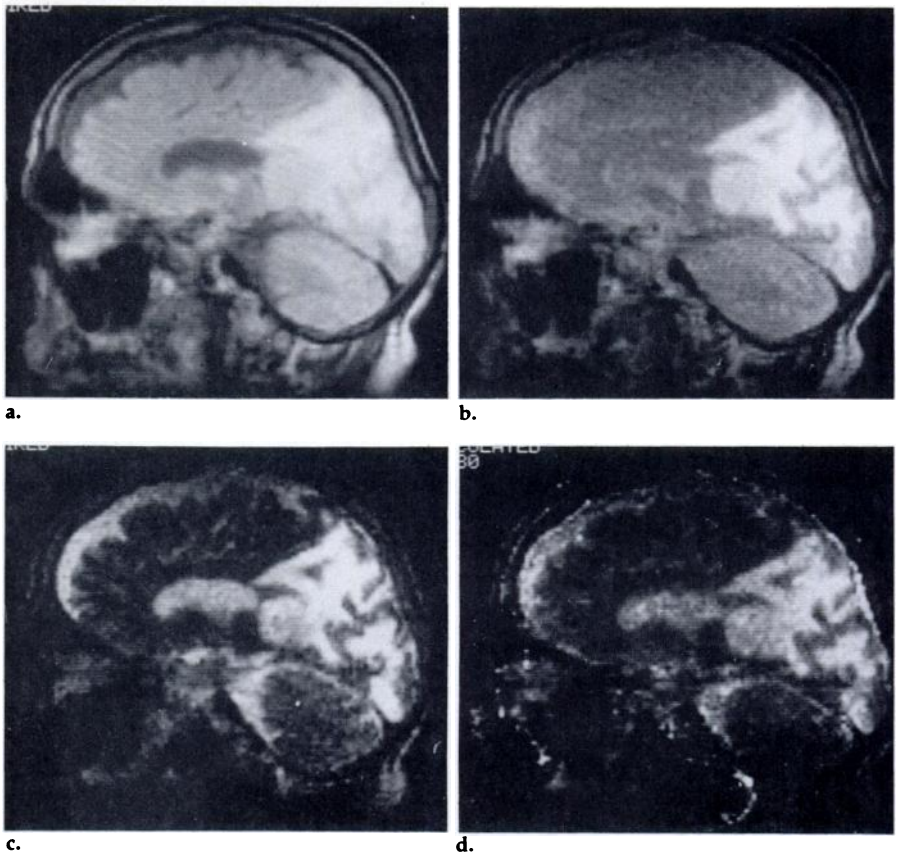

Glioblastoma multiforme. (**a**) TR = 1.5 s, TE = 40 ms; (**b**) TR = 1.5 s, TE = 80 ms; (**c**) TR = 1.5 s, TE = 160 ms; (**d**) TR = 1.5, TE = 160 ms, calculated from 40 and 80 ms images. The glioblastoma is more sharply marginated from the contiguous brain when the echo delay is prolonged. The calculated and the acquired images contain diagnostically equivalent information; however, the S/N ratio is lower in calculated images from tissues with longer T2 values.

the lesion and background healthy tissue remains essentially unchanged when the standard error ΔC is taken into account (TABLES I and II). The overall lesion detection confidence ($C/\Delta C$) also remains comparable between acquired late TE images and those synthesized from earlier echoes.

While T2 relaxation has a predictable effect on later echoes, the movement of nuclei in a uniform direction (i.e., flow) has an entirely different effect on the image intensity. In the presence of pulsed magnetic field gradients, nuclei that flow in the direction of the gradient produce relatively low signal intensity in the first echo image because of defocusing but produce somewhat higher signal intensity in the second echo image when the signal is partially refocused (11). Thus, using a first and second echo for calculation purposes, the T2 values are artifactually raised (and often become negative) in the pixels that contain vessels. The extrapolation to later TE values then results in very high intensity values for vessels (Fig. 6). If the nuclei flow out of the image section after excitation but before echo acquisition, the intensity will be low in all echoes, which occurs with rapid arterial flow. In a non-cardiac-gated multisection sequence, however, signals are randomly acquired during both systole and diastole. During diastole, arterial velocities are slower, causing second-echo refocusing and flow artifact in the presence of relatively high pulsatile flow velocity. These flow effects are commonly seen in vascular structure images when new spin-echo images are synthesized.

DISCUSSION

MR imaging has already proved itself sensitive in detecting pathologic conditions. Our routine screening sequence for intracranial pathology (12) utilizes long TR spin-echo imaging, usually at TR = 2 s, with echoes at 28 and 56 ms. Once a lesion is detected, however, it is often difficult to characterize it fully with routine imaging data alone. We have found that certain images at carefully chosen, longer TE times may be useful for further lesion evaluation. The ability to obtain these images has been most useful for tumors and certain types of infarction. Longer

Figure 4

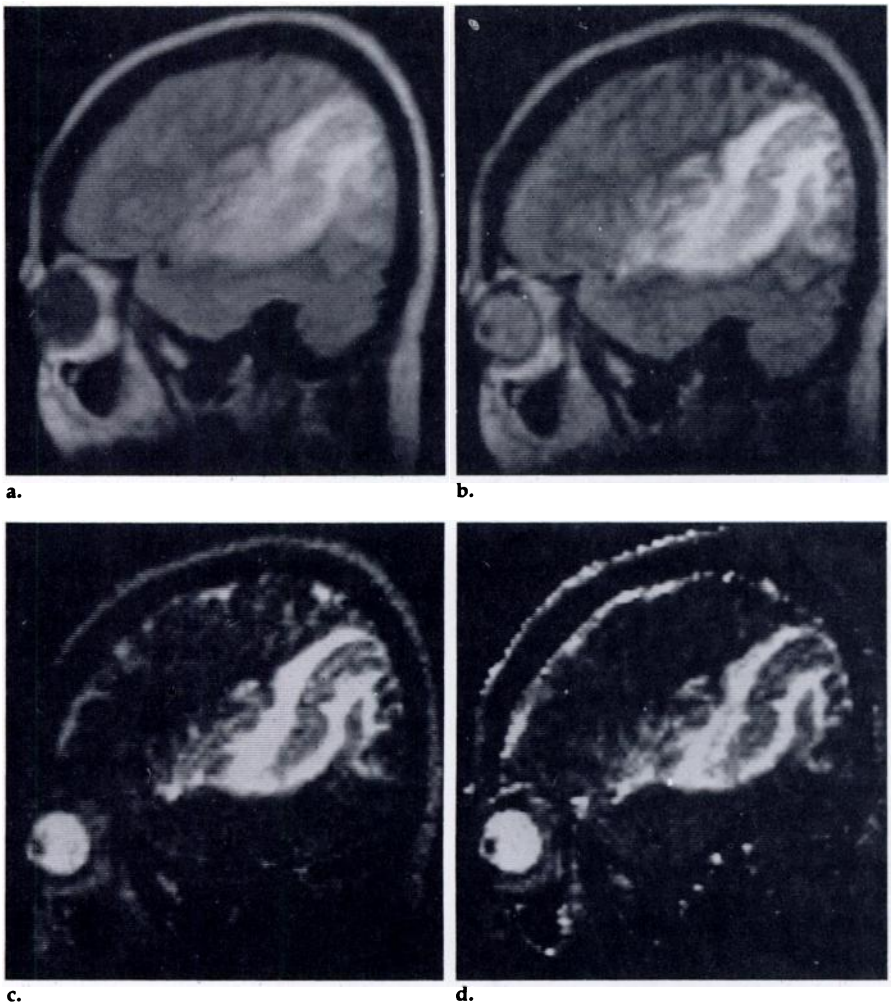

Middle cerebral artery infarct with hemorrhage. (**a**) TR = 1.5 s, TE = 40 ms; (**b**) TR = 1.5 s, TE = 80 ms; (**c**) TR = 1.5 s, TE = 200 ms; (**d**) calculated TR = 1.5 s, TE = 200 ms. Short echo times have better gray-white contrast, which decreases at longer echo delays. However, the infarct is better defined in both calculated and acquired images that have longer echo delays.

Figure 5

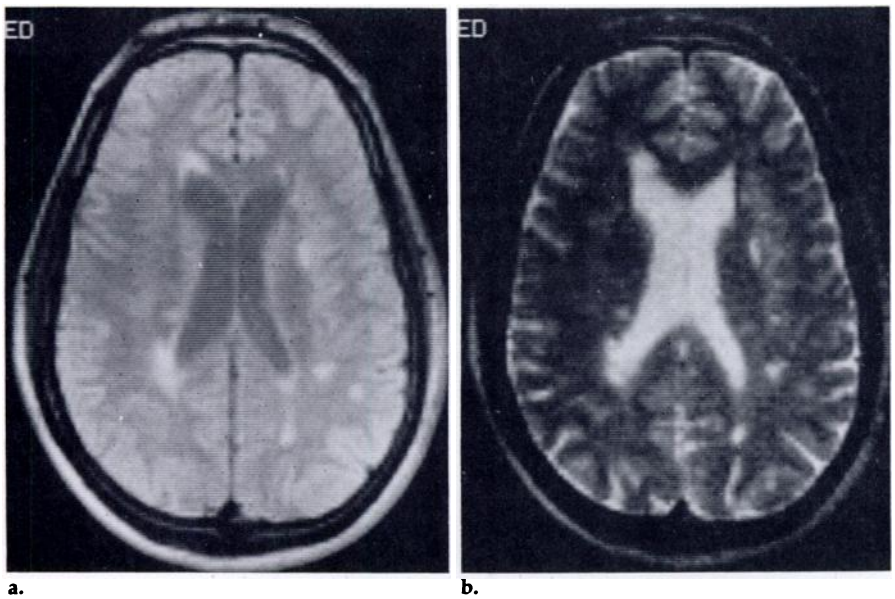

Multiple sclerosis. (**a**) TR = 2.0 s, TE = 40 ms; (**b**) TR = 2.0 s, TE = 160 ms. Multifocal periventricular plaques are clearly defined at relatively short echo times. However, their margins are assimilated by the adjacent CSF and are difficult to distinguish in images obtained at long echo times.

echoes, however, may obscure the correct diagnosis, as in patients with periventricular lesions (e.g., multiple sclerosis) where the augmented intensity of CSF may obscure the interface between lesion and ventricle.

We can obtain multiple spin-echo images prospectively, which has the advantage of better S/N ratios than does retrospective intensity image synthesis. This is done, however, at the price of decreased throughput. We obtained only six contiguous sections, each with five echoes widely spaced in time, in the same imaging time it takes to obtain our routine 20 sections, each with two relatively short echoes, from which longer TE images may be extrapolated.

The comparison of calculated to acquired long TE intensity images shows a remarkable similarity in image contrast predicted by an exponential model of tissue intensity changes. Calculations of contrast between lesions and their backgrounds, and the determination of detection confidence (measured by $C/\Delta C$ and shown in the tables) confirm the subjective impression noted on analysis of multiple examinations. The decrease in confidence of calculated images follows S/N ratio changes as predicted by calculations from pairs of echoes (Fig. 1). It shows that the confidence in the acquired data, and subsequently in the calculated images derived from these data, depends highly on TE. By selecting two relatively short TE times, as we have done, the relative S/N ratio in tissues with shorter T2 in each resultant image is higher, and extrapolated images will be more accurate and less noisy. In addition, retrospective calculation offers more flexibility in the choice of TE values. With longer TE times during data acquisition, the number of sections that can be obtained during any multisection sequence will decrease, further reducing clinical utility.

Intravascular blood flow will be visualized on calculated intensity images in a manner different from that on acquired images. This flow artifact yields a striking increase in intensity in these regions, with greater contrast between regions of flow and adjacent immobile tissues in calculated images than seen in acquired images at the same TE. This effect may be useful in highlighting venous and arterial structures that may be less well seen on conventional multisection imaging.

Other considerations of molecular diffusion with respect to multiecho imaging are addressed in the Appendix.

In summary, we evaluated acquired spin-echo images in a multiecho, multisection mode using 2D Fourier

Figure 6

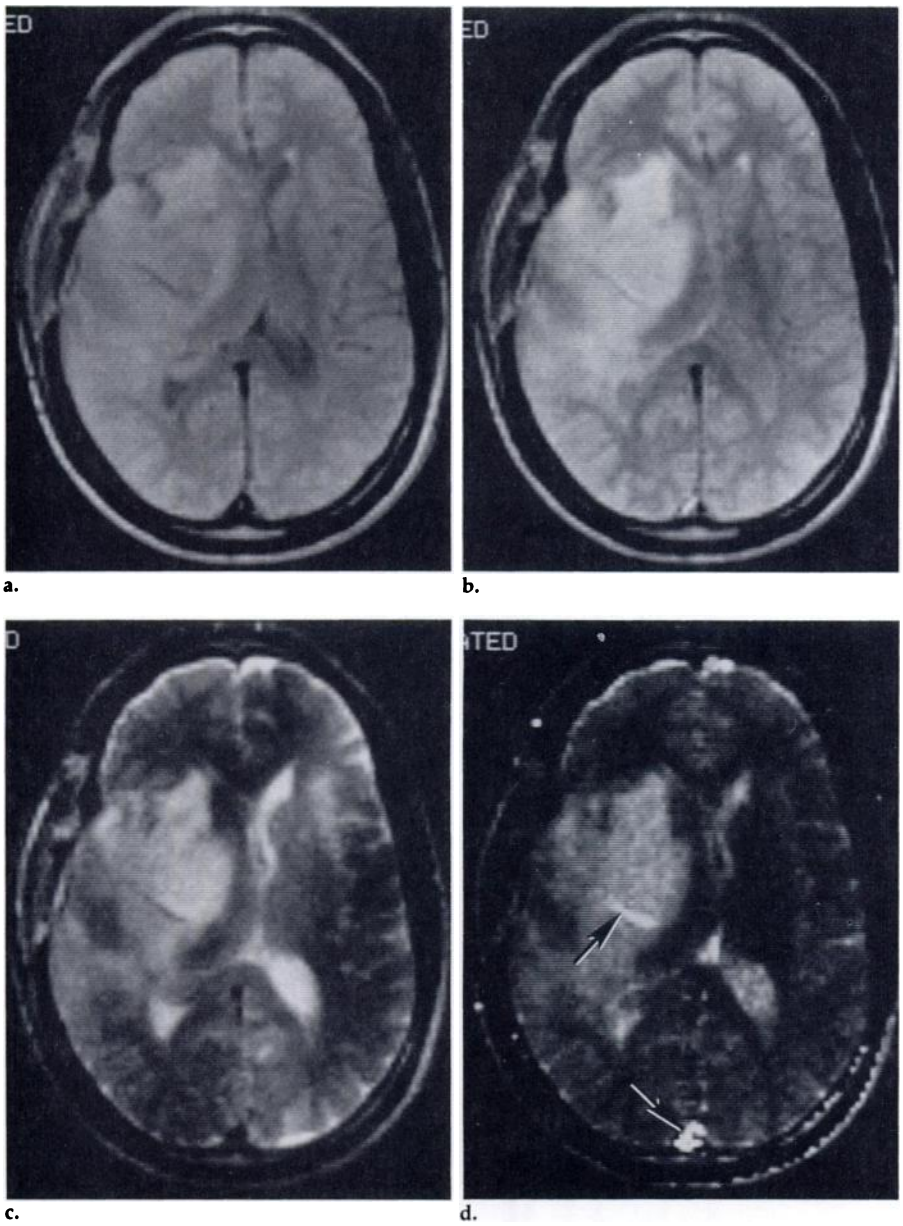

Astrocytoma. (**a**) TR = 2.5 s, TE = 28 ms; (**b**) TR = 2.5 s, TE = 56 ms; (**c**) TR = 2.5 s, TE = 150 ms; (**d**) calculated, TR = 2.5 s, TE = 150 ms. Vascular structures have low signal intensity in the acquired images. Calculated images show vascular structures as high intensity (arrows).

transform techniques, and we explored the utility of synthetic long TE images as an alternative. Both have clinical utility in the analysis and detection of pathologic entities, and both have disadvantages with respect to clinical throughput and S/N ratio considerations. In practice, it may be more expeditious to screen patients with a routine, long TR two-echo sequence, and either add a multiecho sequence or perform retrospective image analysis and synthesis when more information is needed to diagnose complex pathologic conditions.

APPENDIX

As demonstrated by Carr and Purcell (1), signal loss during long TE because of molecular diffusion in static magnetic field heterogeneities can be reduced with a shorter time between consecutive 180° refocusing pulses. This is accomplished by increasing the number of echoes in the pulse sequence out to the long TE. This reduced diffusion effect on signal magnitude depends on the time between RF pulses and is identical in both the acquired late-echo image and the synthetic late-echo image given a constant change in TE between successive images. A single echo (2) at the same long TE will have a much greater time between RF pulses and an apparent shorter spin-spin relaxation time (tissue T2). In all the above cases, the additional effects of magnetic gradient calibration, body motion, and RF heterogeneity may reduce signal magnitude and image intensity more than they reduce diffusion.

In addition to background static magnetic field heterogeneities, relatively strong magnetic gradient pulses are present during the 180° RF pulses for defining section thickness. Because of diffusion, these gradient pulses cause further apparent shortening of tissue T2. This is not like imaging a single section with multiple echoes (3), which does not require these gradient pulses, and consequently the effect of diffusion is less than in multisection imaging.

David A. Feinberg, Ph.D.
University of California, San Francisco
Radiologic Imaging Laboratory
400 Grandview Drive
South San Francisco, California 94080

References

1. Carr HY, Purcell EM. Effects of diffusion on free precession in nuclear magnetic resonance experiments. Phys Rev 1954; 94: 630–638.
2. Hahn EL. Spin echoes. Phys Rev 1950; 80:580–594.
3. Ford J, Bryan RN, Willcott MR. Accurate T2 NMR images. Med Phys 1983; 10(5):642.
4. Crooks LE, Arakawa M, Hoenninger J, et al. Nuclear magnetic resonance whole-body imager operating at 3.5 KGauss. Radiology 1982; 143:169–174.
5. Crooks LE, Ortendahl DA, Kaufman L, et al. Clinical efficiency of nuclear magnetic resonance imaging. Radiology 1983; 146: 123–128.
6. Ortendahl DA, Hylton NM, Kaufman L, et al. Analytical tools for MRI. Radiology 1984; 153:479–488.
7. Meiboom S, Gill D. Modified spin-echo method for measuring nuclear relaxation times. Rev Sci Instrum 1958; 29:688–691.
8. Kumar A, Welti D, Ernst RR. NMR Fourier zeugmatography. J Magnetic Resonance 1975; 18:69–83.
9. Ortendahl DA, Hylton NM, Kaufman L, Crooks LE. Signal-to-noise in derived NMR images. Magnetic Resonance Med 1984; 1: 316–338.
10. Hylton NM, Feinberg D, Ortendahl DA, Crooks LE, Kaufman L, Mills CM. Digital synthesis of the information in multiple echoes (abstr.) Paper presented at the Third Annual Meeting of the Society of Magnetic Resonance in Medicine, New York, August 13–17, 1984.
11. Feinberg DA, Crooks LE, Hoenninger J, Arakawa M, Watts J. Pulsatile blood velocity in human arteries displayed by magnetic resonance imaging. Radiology 1984; 153:177–180.
12. Brant-Zawadzki M, Norman DC, Newton TH, et al. Magnetic resonance of the brain: the optimal screening technique. Radiology 1984; 152:71–77.